Imprints of the Frequency-Domain Source Function on Black Hole Ringdown

Aleyna Koro,[1] Andrew Laeuger,[2] Colin Weller,[2] and Yanbei Chen[2]
[1] *Northeastern University, Boston, MA, USA*
[2] *LIGO Laboratory, California Institute of Technology, Pasadena, CA, USA*
(Dated: September 26, 2025)

In recent years, substantial attention has been paid towards gathering physical information from the ringdown portion of gravitational wave (GW) signals from compact object mergers. These studies have generally been interested in inferring astrophysical parameters, such as the masses and spins of the progenitors, from quasinormal mode (QNM) amplitudes and phases. In this work, we investigate whether the structure of the source term which generates the ringdown itself can be extracted from the resulting waveform. In particular, we explore whether applying the ringdown filters of Ma et al. [14] to a ringdown waveform leaves behind a signature characterized by the behavior of the frequency-domain source. Using black hole perturbation theory, we compute frequency-domain Green's function for the radial Teukolsky equation on a Kerr background, employing the numerically stable Generalized Sasaki–Nakamura form. We then apply the frequency-domain filters to nontrivial radial and frequency-domain behavior and analyze whether the filters return signals which can clearly be associated with the form of the source. This framework establishes the tools needed to test whether filtered ringdown waveforms can isolate the imprint of the source, with the goal of extending the analysis to more realistic astrophysical perturbations.

I. INTRODUCTION

A. Background

When two black holes merge, they heavily distort spacetime; this disturbance creates ripples in spacetime that propagate outwards as gravitational waves. General relativity (GR) predicts that a binary black hole merger will produce a gravitational wave signal with three phases: inspiral, merger, and ringdown. The ringdown is the final stage where the remnant black hole settles down into its final state via oscillations known as quasinormal modes (QNMs), which dominate this phase. However, additional components such as power-law tails may appear at late times. The ringdown can be treated as a perturbation of the Kerr spacetime and the gravitational radiation is described by the Teukolsky equation [20]. Like a plucked guitar string vibrating, the black hole quasinormal oscillations occur with specific frequencies and decay times. These QNM frequencies are completely determined by the final black hole's mass and spin, which is consistent with the no hair theorem [7, 10]. When a source perturbs a black hole, the resulting radiation is the ringdown predicted by perturbation theory that separates the ringdown as a prompt response, QNM excitation, and a power-law tail. The prompt response, also known as the precursor, is the initial burst of radiation that travels directly from the source to the observer, while the QNM excitations arises from radiation that backscatters off the black hole's curved spacetime geometry (the effective potential barrier) before reaching the observer [11, 15]. The power-law tail is the radiation that backscatters off the space-time curvature far from the black hole.

The first observation of gravitational waves came from a binary black hole merger on September 14, 2015 (GW150914) [1]. This detection confirmed the existence of QNMs within the ringdown phase through detailed modeling of the waveform. Since then, several studies have focused specifically on analyzing the ringdown of GW150914, using it to test general relativity and extract the properties of the remnant black hole [3, 4, 6]. Historically, extracting QNM amplitudes and phases has been the primary method of analyzing the ringdown [8, 21]. Sizheng Ma et al. [14] introduced frequency-domain filters designed to aid in the analysis of black hole ringdown signals. Two filters are considered in their work: the rational filter, which targets specific quasinormal modes, and the full filter, which removes the entire QNM content of the signal.

B. Motivation

Many ringdown analyses focus on inferring the remnant black hole's properties[5], understanding how the QNMs are excited[17], and testing GR [1, 5]. These analysis typically assume a known source of perturbation from numerical simulations, such as a plunging particle or a merging black hole, and aim to compute the resulting waveform rather than infer details about the source itself. Therefore, the question arises to whether we can extract information about the source itself from the ringdown. Specifically, intermediate sources that are not studied in current literature and are more complicated than the Dirac delta function but less complex than one describing a black hole merger. Extracting the behavior of the source from the ringdown could provide a better understanding of the environmental signature around a black hole and could offer a much stronger test of GR.

Similarly, there has been little investigation into the use of ringdown filters. This study will help determine whether ringdown filters could be a useful tool in ringdown data analysis for improving parameter estimation and testing general relativity.

This paper is organized as follows. In Sec. II, we review the homogeneous Teukolsky/Generalized Sasaki-Nakamura (GSN) setup and validate the Green's function construction. In Secs. III and IV, we apply the ringdown filters to toy sources, Dirac delta and Gaussian functions. In Sec. V, we use a Lorentzian frequency–domain source designed to preferentially excite QNMs, considering centers at $\mathrm{Re}(\omega_{\ell mn})$ and at the full complex $\omega_{\ell mn}$.

In this work we use geometrized units $G = c = 1$ and normalize the black hole mass to $M = 1$. The black hole spin is $a = 0.7$,the spin weight is $s = -2$, and we focus on the dominant $(\ell, m) = (2, 2)$ modes.

II. PERTURBATIONS TO ROTATING BLACK HOLES

A. Homogeneous Solutions to the Teukolsky and Sasaki-Nakamura Equations

The ringdown portion of a compact merger waveform is commonly modeled via black hole perturbation theory, wherein the post-merger gravitational waves are treated as a perturbation to the Kerr metric which describes the remnant BH. The gravitational radiation emitted by this Kerr BH can be described by the Teukolsky equation [20]. The Teukolsky equation is a second-order linear partial differential equation that describes how a perturbation to a rotating black hole evolves. The equation can be decomposed into a radial and angular part shown in Eqs. 1 and 2.

Due to the separability and the symmetries of the Kerr background this reduces the problem to two coupled ordinary differential equations: an angular equation for the spin-weighted spheroidal harmonics and a radial equation for the wave propagation. The angular equation is of Sturm–Liouville type, with the spin-weighted spheroidal harmonics as eigenfunctions and the separation constant λ as the corresponding eigenvalue. The radial equation, supplemented with boundary conditions of purely ingoing waves at the horizon and purely outgoing waves at infinity allows solutions for only a discrete set of complex frequencies ω_{lmn} [16]. These frequencies correspond to the black hole's QNMs.

$$\begin{aligned}&\Delta^{-s}\frac{d}{dr}\left(\Delta^{s+1}\frac{dR}{dr}\right)\\&+\left(\frac{K^2-2is(r-M)K}{\Delta}+4is\omega r-\lambda\right)R=0\end{aligned}\tag{1}$$

$$\begin{aligned}\frac{1}{\sin\theta}\frac{d}{d\theta}\left(\sin\theta\frac{dS}{d\theta}\right)+\Big(a^2\omega^2\cos^2\theta-\frac{m^2}{\sin^2\theta}-2a\omega s\cos\theta\\-\frac{2ms\cos\theta}{\sin^2\theta}-s^2\cot^2\theta+s+A\Big)S=0\end{aligned}\tag{2}$$

In Eq. 1, $\Delta = r^2 - 2Mr + a^2$ is the horizon function of the Kerr metric, where M is the black hole mass and a is its spin parameter. The function $K(r) = (r^2 + a^2)\omega - am$, where ω is the Fourier frequency and m is the azimuthal quantum number. The separation constant $\lambda = A + a^2\omega^2 - 2am\omega$ arises from angular separation(A) and is related to the eigenvalue of the spin-weighted spheroidal harmonics(S). The function $R(r)$ is the radial part of the perturbation. s is the spin weight of the perturbation. $s = -2$ is used in later calculations to describe outgoing gravitational radiation.

B. Sourced Solutions

In order to understand the behavior of a source from ringdown, first the sourced waveform must be computed using the Green's function. The Green's function is the response of the black hole spacetime to a source, $S_{lm}(r'_*, \omega)$. The frequency-domain solution $R(r)$ is converted to the time domain via an inverse Fourier transform, yielding $\psi(t,r)_{\mathrm{hom}}$, the time-domain Teukolsky radial function. In our case, $\psi(t,r)_{\mathrm{hom}}$ is the direct output of the Green's-function inversion. It is not directly the metric perturbation $h_{\mu\nu}$. A metric-reconstruction procedure, such as the Chrzanowski-Cohen-Kegeles(CCK) formalism, is required to obtain the observable gravitational wave strain, $h(t,r)$[2, 9].

$$\psi(t,r_*)_{\mathrm{hom}}=\sum_{\ell,m}\int\frac{d\omega}{2\pi}\,e^{-i\omega t}\int dr'_*G_{\ell m}(r_*,r'_*,\omega)\,S_{\ell m}(r'_*,\omega).\tag{3}$$

We then construct the factorized Green's function, $G_{lm}(\omega, r_*, r'_*)$:

$$\begin{aligned}G_\ell(\omega,r_*,r'_*)=\frac{1}{W_\ell(\omega)}\Big[\,&\theta(r_*-r'_*)\,R_\ell^{\mathrm{in}}(\omega,r'_*)\,R_\ell^{\mathrm{up}}(\omega,r)\\&+\theta(r'_*-r_*)\,R_\ell^{\mathrm{in}}(\omega,r_*)\,R_\ell^{\mathrm{up}}(\omega,r'_*)\Big],\end{aligned}\tag{4}$$

where θ is the Heaviside function and R^{in} and R^{up} are the homogeneous solutions to the radial Teukolsky equation with ingoing boundary conditions at the horizon and outgoing boundary conditions at infinity, respectively. We obtain these solutions using Rico K. Lo's `Julia` package [12] that uses the Generalized Sasaki Nakamura (GSN) formalism to solve the radial part of the homogeneous Teukolsky equation from Eq. 1 [12]. The GSN formalism transforms the Teukolsky equation into an equation that excludes the case for outgoing radiation. As a result, the equation is more numerically stable as seen in Fig. 1 where the amplitude in the GSN solution 1a retains a constant amplitude while the Teukolsky solution 1b grows rapidly.

With these solutions the Wronskian, $W_\ell(\omega)$, can be

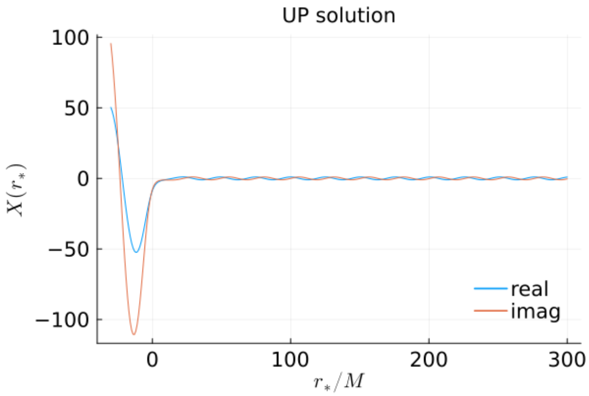

(a) GSN Solution

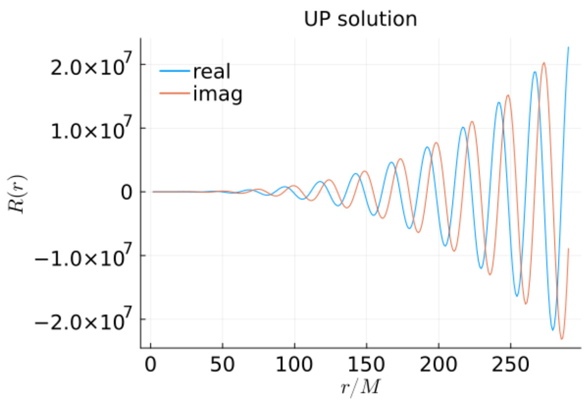

(b) Teukolsky Solution

FIG. 1: GSN and Teukolsky Solution Comparison [12].

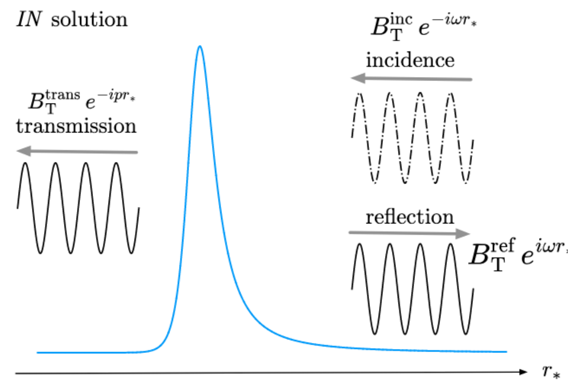

(a) IN solution

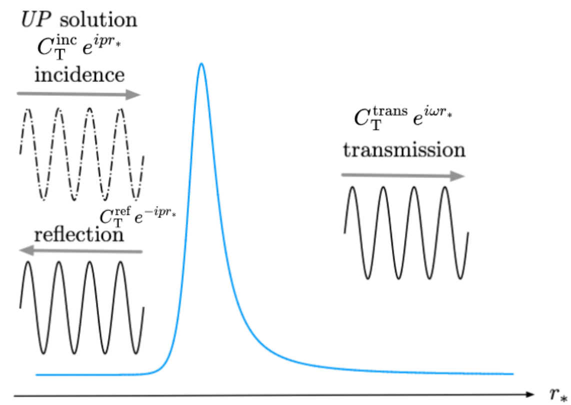

(b) UP solution

FIG. 2: Amplitudes of the radial Teukolsky solutions for (a) IN and (b) UP solutions [12].

calculated in two ways:

$$\mathcal{W}_R = \Delta^{s+1}\left(R^{\rm in}\frac{R^{\rm up}}{dr_*} - R^{\rm up}\frac{R^{\rm in}}{dr_*}\right) \tag{5}$$

$$\mathcal{W}_R = 2i\omega C_{\rm T}^{\rm trans} B_{\rm T}^{\rm inc} \tag{6}$$

Where $C_{\rm T}^{\rm trans} = 1$. In Eq. 5, the radial solutions to the Teukolsky equations and their derivatives with respect to r can be used. We compute these derivatives using the `ForwardDiff` Julia package [18]. In Eq. 6, the incidence and transmission amplitudes of the incoming and outgoing waves are used. A physical depiction of these amplitudes is shown in Fig. 2. For ease, in waveform computations Eq. 6 is used.

C. Filters

Recently, the ringdown filters of Ma et al.[14] have been proposed as an alternative approach to the standard practice of fitting QNM amplitudes for analyzing ringdown data. These filters are already seeing some use in searching for subdominant modes in ringdown data, benefiting from the fact that they do not rely whatsoever on statistical fits of the amplitudes of dominant modes [13, 14]. The first of the two filters, the "rational" filter, is given for a single QNM frequency $\omega_{\ell mn}$ by

$$\mathcal{F}_{\ell mn}(\omega) = \frac{\omega - \omega_{\ell mn}}{\omega - \omega^*_{\ell mn}}. \tag{7}$$

These QNM frequencies correspond to the poles of the Green's function, and in this work, we compute them using the `qnm` Python package [19].

This filter mirrors a ringdown component at frequency ω_{lmn} backwards across its starting time, removing it from the ringdown signal while maintaining the total waveform power. Multiple QNMs can be filtered simultaneously through a product of rational filters. A QNM contribution at frequency $\omega_{\ell' m' n'}$ which is not directly filtered out by $\mathcal{F}_{\ell mn}$ will see its amplitude in the time-domain ringdown reduced by $\mathcal{F}_{\ell mn}(\omega_{\ell' m' n'})$.

The full filter, on the other hand, is given by:

$$\mathcal{F}^D_{\ell m} = \frac{D^{\rm out}_{\ell m}(\omega)}{(D^{\rm out}_{\ell m}(\omega))^*}, \tag{8}$$

where $D^{\rm out}_{\ell m}(\omega)$ is the amplitude of the outgoing wave at the horizon obtained from the radial Teukolsky solution with "up" (i.e., purely outgoing at infinity) boundary conditions. In other words, $D^{\rm out}_{\ell m}(\omega)$ is the inverse transmissivity of the Kerr spacetime to outgoing waves initiating near the horizon. Near the QNM frequencies, $D^{\rm out}(\omega) \sim (\omega - \omega_{\ell mn})$. So not only should the full filter mirror QNM components backwards across their starting time, like the rational filter, in principle it also removes all QNM frequencies from a given (ℓ, m) harmonic. Instead of the inverse transmissivity of the "up" solution, we employ the full filter constructed with $B^{\rm inc}_{\ell m}(\omega)$, which is the inverse transmissivity of the radial solution with "in" (i.e., ingoing at the horizon) boundary conditions. The two coefficients are related to one another by a simple factor [12][1]:

$$B^{\rm inc}_{\ell m}(\omega) = \frac{(\omega - m\Omega_H)(r_+^2 + a^2) + 2i(r_+ - 1)}{\omega} D^{\rm out}_{\ell m}(\omega). \tag{9}$$

III. ANALYSIS OF DIRAC-DELTA SOURCE FUNCTION WAVEFORMS

As a first step, we use a Dirac-delta source in the radial domain, which acts as a toy model. This simple setup lets us validate our framework before moving to more complicated sources. Assuming the source radius r'_* is always smaller than the observer radius r_*, which is justified since the detector is always located far from the black hole, so the observer radius r_* lies well outside the source radius r'_*, the Green's function in Eq.10 reduces to

$$G(r_*, r'_*, \omega) = \frac{R^{\rm in}(r'_*) R^{\rm up}(r_*)}{W(\omega)}. \tag{10}$$

For a Dirac-delta radial source profile, the sourced waveform is simply equal to the time-domain Green's function evaluated at a particular choice of source radius r'_*. With this in mind, our analysis in fact aims to confirm whether $R^{\rm up}$ satisfies the homogeneous Teukolsky equation.

A. Unfiltered

Using $a = 0.7, l = 2, m = 2, s = -2$, the sourced waveform in the time domain from Eq.(3) is computed via manual inverse Fourier Transform for a Dirac delta source function. The plots in Fig. 3 show $\psi(t, r_*)_{\rm hom}$ for a various range of source locations.

Since the source here is modeled as a Dirac delta function which is point-like in space and instantaneous in time, the prompt response requires infinitely large frequencies to model properly; thus only the ringdown appears. In this setup, the source and initial data should be regarded as different quantities, so we do not expect a prompt response. Instead, the waveform exhibits a ring up and ringdown which is sufficient for validating the Green's function construction.

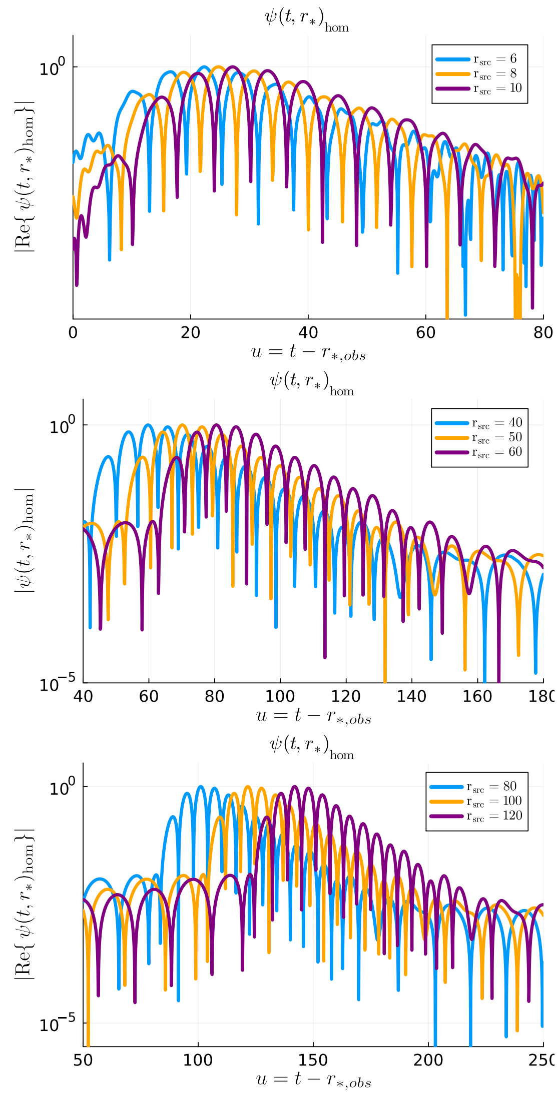

FIG. 3: Comparison of waveforms for various source locations for delta source function.

When the source is moved farther away from the black hole, we expect the onset of the ringdown to be delayed by the radial shift. This is because the inward-traveling part of the perturbation must first propagate from the source to the near-horizon region to excite the quasinormal modes, and then the resulting radiation must travel back out to the observer. The plots confirm this expectation: for example, shifting the source location from $r'_* = 40$ to $r'_* = 50$ delays the ringdown by 10 in the retarded time ($u = t - r_{*,\rm obs}$).

[1] Note that $D^{\rm out}$ is designated as $C^{\rm inc}$ in the referenced paper.

B. Filtered

To investigate how specific quasinormal modes contribute to the overall ringdown signal, we apply the filters described in Section II C to the unfiltered waveforms obtained above for a delta source. The goal is to remove the targeted modes from the signal. Two types of filters are considered: the full filter, which is constructed from the transmissivity of the black hole, and the rational filter, which is built from a set of QNMs.

Using the unfiltered waveforms computed for $a = 0.7, l = 2, m = 2, s = -2$, we apply the full filter described in Eq. 8 to remove the full set of QNMs as seen from the red curve in Fig. 4.

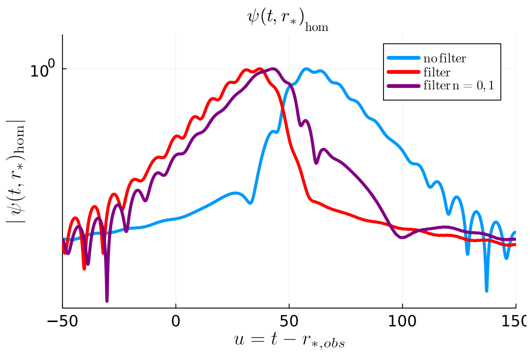

FIG. 4: Full filter and rational filter applied to delta sourced waveform for $r'_* = 40$

As expected, applying the full filter removes the quasinormal ringing quite effectively, leaving the waveform quite small in magnitude in the region where the ringing previously lay. The residual signal corresponds to the non-physical time reversed counterpart of the removed QNM, which is a mathematical consequence of the filtering procedure.

In the purple curve in Fig. 4, we apply rational filters to remove the fundamental ($n = 0$) first overtone ($n = 1$) from the delta source waveform. The filtered signal shows strong suppression of the late-time portion, consistent with the dominance of the fundamental mode in this regime. At earlier times, the overtone contribution is also reduced, leading to a lower overall amplitude compared to the unfiltered case. The waveform is not completely suppressed, indicating that higher overtones and other components of the response continue to contribute at early times. These results confirm that the rational filter correctly targets and removes the chosen QNM from the signal.

IV. ANALYSIS OF EXTENDED SOURCE FUNCTION WAVEFORMS

Having constructed the Green's function and filtering framework for a Dirac delta source function successfully, we now dedicate this section to investigating spatially extended source functions.

For the sake of making the problem amenable to application of physical intuition, we begin by considering a wave packet which appears somewhere in the radial domain at $t = 0$ and then propagates under the Teukolsky equation. Because the black hole is unperturbed prior to the disturbance of the source, the waveform must vanish for $t < 0$. Physically, no radiation can be observed before the perturbation occurs. To enforce this causality condition, we define the Fourier transform with lower integration limit $t = 0$ rather than $t = -\infty$, ensuring that only the causal response of the black hole to the initial perturbation is included.

Beginning with the time-domain Teukolsky equation,

$$\left(\partial_t^2 - \partial_x^2 + V(x)\right)\Psi(t, x) = 0, \tag{11}$$

we apply the Fourier transform

$$\tilde{\Psi}(\omega, x) = \int_0^\infty \Psi(t, x)\, e^{i\omega t}\, dt. \tag{12}$$

Integrating by parts gives

$$\int_0^\infty (\partial_t^2 \Psi)\, e^{i\omega t}\, dt = \left[\partial_t \Psi\, e^{i\omega t}\right]_0^\infty - i\omega\left[\Psi(t, x) e^{i\omega t}\right]_0^\infty + (i\omega)^2 \tilde{\Psi}(\omega, x). \tag{13}$$

Assuming the field vanishes as $t \to \infty$, only the initial data at $t = 0$ survives. For initial conditions $\Psi(0, x) = \Psi_0(x)$ and $\partial_t \Psi(0, x) = 0$, this reduces to

$$\int_0^\infty (\partial_t^2 \Psi)\, e^{i\omega t}\, dt = i\omega \Psi(0, x) - \omega^2 \tilde{\Psi}(\omega, x). \tag{14}$$

The Fourier-transformed equation then becomes

$$\left(-\partial_x^2 - \omega^2 + V(x)\right)\tilde{\Psi}(\omega, x) = -i\omega \Psi(0, x), \tag{15}$$

which shows that the effective source term is determined directly by the initial data.

In particular, assuming the initial data is described by a Gaussian with center $r_{0,*}$ and width σ, the effective frequency-domain source is

$$S(r_{0,*}, \sigma; r_*, \omega) = -i\omega \frac{1}{\sigma\sqrt{2\pi}} \exp\left(-\tfrac{1}{2}\frac{(r_* - r_{0,*})^2}{\sigma^2}\right). \tag{16}$$

A. Unfiltered

For the Gaussian source function, the unfiltered waveforms exhibit a ringdown. Usually, we would expect a prompt response that is the radiation from the source to the observer without significant scattering. However, in our construction the prompt response is not visible because the $-i\omega$ factor from the Fourier transform cancels against the Wronskian contribution at large frequencies, so in principle the integral which generates the prompt response has support at infinitely large frequencies, a result which is not amenable to numerical integration. Since our study focuses on the ringdown, we do not attempt to capture the prompt response. As expected, shifting the source location r'_* produces a corresponding delay in the onset of the ringdown, consistent with the additional travel time for the inward and outward propagating waves.

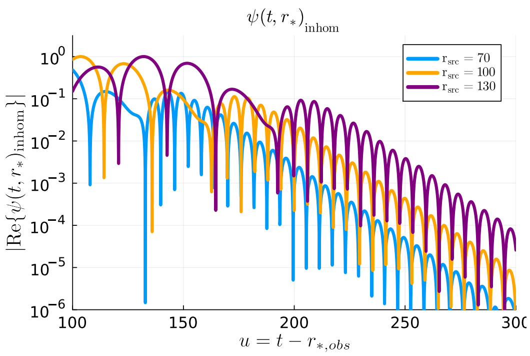

FIG. 5: Comparison of waveforms for various source locations for Gaussian source function.

B. Filtered

Applying the full filter to the Gaussian source waveform (red curve) shown in Fig. 4 removes the quasinormal ringing just as in the delta case. The late-time oscillations are strongly suppressed, and the resulting signal is much smaller in magnitude over the time interval where the QNMs previously dominated.

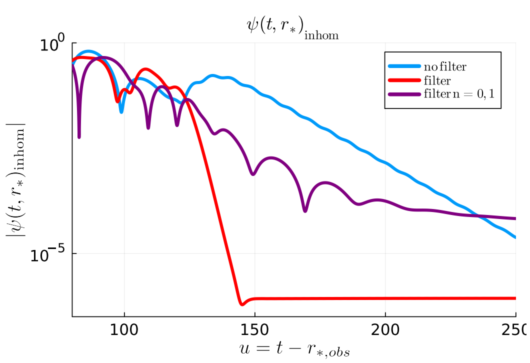

FIG. 6: Full and rational filter applied to Gaussian function centered at $r'_* = 60$

The purple curve in Fig. 4, the rational filter is applied to remove the fundamental($n = 0$) and first overtone($n = 1$) from the Gaussian source waveform and again reduces the waveform amplitude in the expected regions. The late-time signal is strongly suppressed due to the removal of the dominant fundamental mode, while the earlier part of the waveform shows reduced amplitude from suppressing the overtone.

These results show that the rational filter correctly targets the chosen QNMs while leaving behind contributions from higher overtones.

V. ANALYSIS OF LORENTZIAN SOURCE FUNCTION WAVEFORMS

After exploring simple toy sources such as the Dirac delta and Gaussian functions, we consider a toy model designed to preferentially excite a QNM. To achieve this, we use a frequency-domain Lorentzian distribution. In the following subsections, we first analyze the case where the Lorentzian is centered at $\text{Re}(\omega_{\ell nm})$, and then extend to the case where it is centered at the full complex QNM frequency $\omega_{\ell nm}$.

A. Source Centered at Re($\omega_{\ell mn}$)

This source is modeled as a Lorentzian distribution in the frequency domain, multiplied by a radial box function. The Lorentzian is centered at the real part of the target QNM frequency, $\text{Re}(\omega_{\ell nm})$, in attempts that the source preferentially excites oscillations at that mode. The source takes the form:

$$S(r_*, \omega) = B(r'_*) \times f(\omega) \tag{17}$$

Where $B(r'_*)$ is a smoothly tapered radial box function and $f(\omega)$ is the Lorentzian distribution centered at $\text{Re}(\omega_{\ell nm})$ is given by

$$f(\omega) = \frac{1 + 2\gamma_n}{2\pi\left(\gamma_n + \gamma_n^2 + (\omega - \text{Re}\left(\omega_{22n}\right))\left(i + \omega - \text{Re}\left(\omega_{22n}\right)\right)\right)} \tag{18}$$

We set γ_n, the width of the distribution, as

$$\gamma_n = \frac{1}{3}(\text{Re}(\omega_{22\text{n}}) - \text{Re}(\omega_{22\text{n}+1})), \tag{19}$$

where ω_{22n} and ω_{22n+1} denote the QNM frequencies for $\ell = m = 2$ with overtone indices n and $n+1$ respectively, in an attempt to reduce overlap between the different sources at the QNM frequencies. We normalize $f(\omega)$ here so that its integral over all ω is 1.

Fig. 7 shows the resulting ringdown waveforms when the Lorentzian source is peaked at the real part of the fundamental ($n = 0$) and overtone frequencies ($n = 1, 2$). Despite the sources being centered at different QNMs, the waveforms all exhibit nearly identical ringdown behavior. Fig. 8 shows that effect of applying the rational filter to remove the fundamental mode still results in the waveforms peaked at different $\text{Re}(\omega_{\ell nm})$ to be identical.

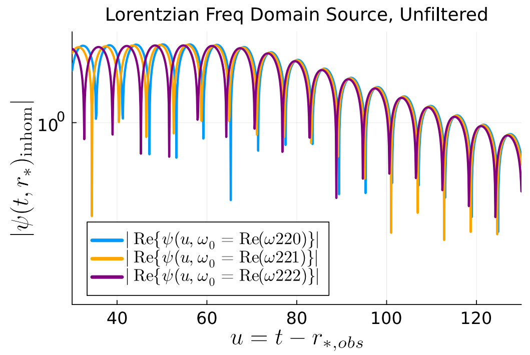

FIG. 7: Unfiltered Lorentzian Centered at $\mathrm{Re}(\omega_{\ell nm})$

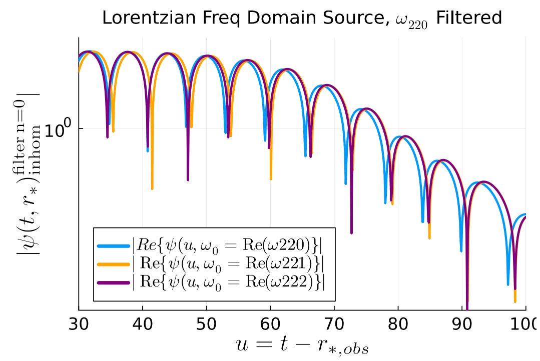

FIG. 8: Filtered $n = 0$ mode for Lorentzian source centered at $\mathrm{Re}(\omega_{\ell nm})$

These similarities can be understood by considering the QNM amplitudes. In general, the amplitude of a QNM excitation may be written schematically as

$$A_{\ell mn} \sim E(\omega_{\ell mn}), S_{\ell' m' n'}(\omega_{\ell mn}) \tag{20}$$

Where $E(\omega_{\ell mn})$ is the excitation coefficient of the black hole which is a property of the background spacetime, independent of the source. $S_{\ell' m' n'}$ is the source term evaluated at the QNM frequency. Table I shows the source functions centered at different real part of the QNMs and evaluated at several QNM frequencies. The values are all very similar, regardless of where the Lorentzian is centered. This explains why the ringdowns in Figs. 7 and 8 appear identical.

$S_{\ell' m' n'}(\omega_{\ell mn})$	ω_{220}	ω_{221}	ω_{222}
$S_{220}(\omega_{\ell mn})$	$2.05356 - 0.0i$	$0.8497 + 0.0264i$	$0.6484 + 0.0150i$
$S_{221}(\omega_{\ell mn})$	$1.9527 - 0.2297i$	$0.8419 - 0.0i$	$0.6458 + 0.0096i$
$S_{222}(\omega_{\ell mn})$	$1.7292 - 0.5580i$	$0.8306 - 0.0464i$	$0.6438 - 0.0i$

TABLE I: Values of the source function $S_{\ell' m' n'}(\omega_{\ell mn})$ evaluated at different QNM frequencies.

We conclude that centering the source at the real part of a QNM frequency for this source function is insufficient to preferentially excite a single mode. In the next section, we investigate whether we can preferentially excite a mode by centering the source at the full complex QNM frequency.

B. Source Centered at $\omega_{\ell mn}$

The source term has a similar set up as in Eq. 17, but $f(\omega)$ is

$$f(\omega) = \frac{1 + 2\gamma_n}{2\pi\Big[\gamma_n + \gamma_n^2 + (\omega - \omega_{22n})\big(i + \omega - \omega_{22n}\big)\Big]}. \tag{21}$$

Where the Lorentzian is peaked at both the real and imaginary parts of the QNM. The motivation is that by driving the source exactly at the QNM frequency the perturbation should preferentially excite that mode. Fig. 9a shows more preferential excitation compared to the real-centered case. This is because the source pole coincides with the pole of the Green's function, creating a double pole. In the time domain, this adds an extra factor of t, which produces a linear growth before the exponential decay represented by the dotted red curve. Physically, this corresponds to resonant amplification of the QNM.

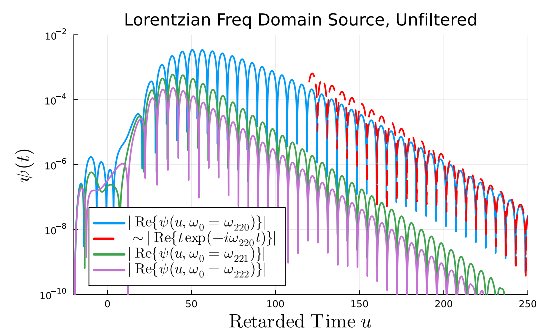

(a) Unfiltered Lorentzian centered at $\omega_{\ell nm}$.

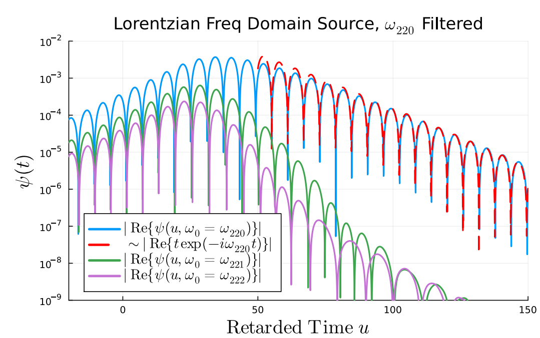

(b) Filtered $n = 0$ mode for Lorentzian source centered at $\omega_{\ell nm}$.

FIG. 9: Comparison of unfiltered (top) and $n = 0$ rational-filtered (bottom) waveforms for Lorentzian sources centered at $\omega_{\ell nm}$.

The resulting waveforms show that the targeted mode is strongly enhanced. However, this setup also contaminates the ringdown because the source continues to drive oscillations at the same frequency while the black hole is simultaneously trying to decay in its natural QNM ringing. As a result, the waveform is no longer a clean, freely decaying oscillation. When the rational filter is applied in Fig. 9b,the rational filter reduces but does not eliminate the fundamental mode. This is expected here because the source itself continues to inject power so the filtered signal still contains a driven component at the same frequency in addition to the black hole's natural frequency response.

Therefore, while centering the source at the full QNM frequency does lead to preferential excitation, the ongoing influence of the source prevents the signal from being interpreted as a pure ringdown.

VI. CONCLUSION

In this work so far, we developed a framework to investigate whether information about the perturbing source can be extracted from the black hole ringdown signal. The approach is based on constructing the homogeneous Green's function from the radial Teukolsky equation using the numerically stable GSN formalism, and validating it through consistency checks on the Wronskian. This framework was first applied to a simple Dirac delta source function. As expected, moving the source location delayed the onset of the ringdown by approximately the radial shift in retarded time.

For the Gaussian source, the waveforms exhibited a clear ringdown but no prompt response, since the effective $-i\omega$ source factor and the Wronskian suppress low-frequency contributions and resolving the prompt piece would require integration to higher frequencies. As with the delta case, shifting the source produced the expected radial delay, and both the full and rational filters successfully suppressed the QNM contributions.

We then turned to Lorentzian frequency-domain sources designed to excite specific modes. When centered at $\mathrm{Re}(\omega_{\ell mn})$, the resulting ringdowns were nearly identical across different centers since the amplitudes are governed by the source evaluated at the complex QNM frequency and those values were very similar. By contrast, when centered at the full complex $\omega_{\ell mn}$, we observed preferential excitation of the target mode but also source contamination. In this case, the source continues driving at the QNM frequency while the black hole simultaneously attempts to decay, producing a waveform that is no longer a clean, freely decaying oscillation. Because of the resulting double pole, the rational filter cannot fully remove the fundamental mode.

Going forward, a natural extension is to use these tools to test general relativity. For example, by checking whether overtone amplitudes and frequencies obey the no-hair theorem by using filters. We also aim to move beyond toy models and investigate more realistic perturbations such as accretion disks or matter clouds, to assess whether astrophysical environments leave measurable imprints on the ringdown.

VII. ACKNOWLEDGMENTS

This work was supported by the National Science Foundation Research Experience for Undergraduates (NSF REU) program, the LIGO Laboratory Summer Undergraduate Research Fellowship program (NSF LIGO), and the California Institute of Technology Student-Faculty Programs. I would also like to thank my mentors Andrew Laeuger and Colin Weller for their continued support and guidance. A.L. acknowledges support by the Fannie and John Hertz Foundation.

[1] B. P. Abbott et al. Observation of Gravitational Waves from a Binary Black Hole Merger. *Phys. Rev. Lett.*, 116(6):061102, 2016.

[2] Paul L. Chrzanowski. Vector potential and metric perturbations of a rotating black hole. *Phys. Rev. D*, 11:2042–2062, Apr 1975.

[3] Alex Correia, Yi-Fan Wang, Julian Westerweck, and Collin D. Capano. Low evidence for ringdown overtone in gw150914 when marginalizing over time and sky location uncertainty, 2024.

[4] Roberto Cotesta, Gregorio Carullo, Emanuele Berti, and Vitor Cardoso. Analysis of ringdown overtones in gw150914. *Phys. Rev. Lett.*, 129:111102, Sep 2022.

[5] Matthew Giesler, Maximiliano Isi, Mark A. Scheel, and Saul A. Teukolsky. Black hole ringdown: The importance of overtones. *Phys. Rev. X*, 9:041060, Dec 2019.

[6] Maximiliano Isi and Will M. Farr. Revisiting the ringdown of gw150914, 2022.

[7] Maximiliano Isi, Matthew Giesler, Will M. Farr, Mark A. Scheel, and Saul A. Teukolsky. Testing the no-hair theorem with gw150914. *Phys. Rev. Lett.*, 123:111102, Sep 2019.

[8] Xisco Jiménez Forteza, Swetha Bhagwat, Paolo Pani, and Valeria Ferrari. Spectroscopy of binary black hole ringdown using overtones and angular modes. *Physical Review D*, 102(4), August 2020.

[9] Lawrence S. Kegeles and Jeffrey M. Cohen. Constructive procedure for perturbations of spacetimes. *Phys. Rev. D*, 19:1641–1664, Mar 1979.

[10] E. W. Leaver and Subrahmanyan Chandrasekhar. An analytic representation for the quasi-normal modes of kerr black holes. *Proceedings of the Royal Society of London. A. Mathematical and Physical Sciences*, 402(1823):285–298, 1985.

[11] Edward W. Leaver. Spectral decomposition of the perturbation response of the schwarzschild geometry. *Phys. Rev. D*, 34:384–408, Jul 1986.

[12] Rico K. L. Lo. Recipes for computing radiation from a Kerr black hole using a generalized Sasaki-Nakamura formalism: Homogeneous solutions. *Phys. Rev. D*, 110(12):124070, 2024.

[13] Neil Lu, Sizheng Ma, Ornella J. Piccinni, Ling Sun, and Eliot Finch. Statistical identification of ringdown modes with rational filters. 5 2025.

[14] Sizheng Ma, Keefe Mitman, Ling Sun, Nils Deppe, François Hébert, Lawrence E. Kidder, Jordan Moxon, William Throwe, Nils L. Vu, and Yanbei Chen. Quasinormal-mode filters: A new approach to analyze the gravitational-wave ringdown of binary black-hole mergers. *Physical Review D*, 106(8), October 2022.

[15] Michele Maggiore. *Gravitational Waves. Vol. 2: Astrophysics and Cosmology.* Oxford University Press, 3 2018.

[16] William H. Press and Saul A. Teukolsky. Perturbations of a Rotating Black Hole. II. Dynamical Stability of the Kerr Metric. *Astrophys. J.*, 185:649–674, October 1973.

[17] Richard H. Price, Sourabh Nampalliwar, and Gaurav Khanna. Black hole binary inspiral: Analysis of the plunge. *Phys. Rev. D*, 93:044060, Feb 2016.

[18] J. Revels, M. Lubin, and T. Papamarkou. Forward-mode automatic differentiation in Julia. *arXiv:1607.07892 [cs.MS]*, 2016.

[19] Leo C. Stein. qnm: A Python package for calculating Kerr quasinormal modes, separation constants, and spherical-spheroidal mixing coefficients. *J. Open Source Softw.*, 4(42):1683, 2019.

[20] Saul A. Teukolsky. Perturbations of a Rotating Black Hole. I. Fundamental Equations for Gravitational, Electromagnetic, and Neutrino-Field Perturbations. *Astrophys. J.*, 185:635–648, October 1973.

[21] Hengrui Zhu, Harrison Siegel, Keefe Mitman, Maximiliano Isi, Will M. Farr, Michael Boyle, Nils Deppe, Lawrence E. Kidder, Sizheng Ma, Jordan Moxon, Kyle C. Nelli, Harald P. Pfeiffer, Mark A. Scheel, Saul A. Teukolsky, William Throwe, Vijay Varma, and Nils L. Vu. Black hole spectroscopy for precessing binary black hole coalescences, 2025.